NSTX-U

NSTX-U is sponsored by the
U.S. Department of Energy Office of Science
Fusion Energy Sciences

Advanced Plasma Shape Control to Enable High-Performance Divertor Operation on NSTX-U

P. J. Vail, E. Kolemen

Princeton University, Princeton, NJ 08540

M. D. Boyer

Princeton Plasma Physics Laboratory, Princeton, NJ 08544

A. W. Welander

General Atomics, San Diego, CA

Presented at the 59th Annual Meeting of the APS Division of Plasma Physics

PRINCETON UNIVERSITY

PPPL

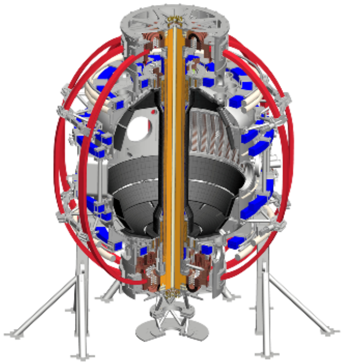

Abstract

This work presents the development of an advanced framework for control of the global plasma shape and its application to a variety of shape control challenges on NSTX–U. Operations in high-performance plasma scenarios will require highly-accurate and robust control of the plasma poloidal shape to accomplish such tasks as obtaining the strong-shaping required for the avoidance of MHD instabilities and mitigating heat flux through regulation of the divertor magnetic geometry. The new control system employs a high-fidelity model of the toroidal current dynamics in NSTX–U poloidal field coils and conducting structures as well as a first-principles driven calculation of the axisymmetric plasma response. The model-based nature of the control system enables real-time optimization of controller parameters in response to time-varying plasma conditions and control objectives. The new control scheme is shown to enable stable and on-demand plasma operations in complicated magnetic geometries such as the snowflake divertor. A recently-developed code that simulates the nonlinear evolution of the plasma equilibrium is used to demonstrate the capabilities of the designed shape controllers. Plans for future real-time implementations on NSTX–U and elsewhere are also presented.

Introduction

Goals of this work

- The use of advanced divertor configurations, such as the snowflake divertor (SFD), is being considered as a possible means of reducing peak heat flux onto divertor surfaces in NSTX-U.
- Develop an algorithm that is capable of real-time control of all divertor configurations of interest in NSTX-U.
- Address primary limitations of the algorithm as previously implemented on DIII-D:
  - Stable control of the SFD-Plus configuration.
  - Recovery from high-field-side to low-field-side SFD-Minus.

  E. Kolemen *et al. J. Nucl. Mater.* (2015).
- Transition to model-based (non-PID) plasma shape control for NSTX-U.

Highlights

- New modeling of X-point position response to PF coil currents.
- PID-based control of the SFD with closed-loop controller tuning using relay feedback.
- Initial development of model-based Linear-Quadratic-Integral control of the plasma shape.

Formalism for plasma shape control modeling

Coupled circuit equations describing dynamics of toroidal currents in coils, passive structures, and plasma.

$$\mathbf{M_{cc}}\,\dot{\mathbf{I}}_\mathbf{c} + \mathbf{M_{cv}}\,\dot{\mathbf{I}}_\mathbf{v} + \dot{\mathbf{\Psi}}_\mathbf{cp} + \mathbf{R_c}\,\mathbf{I_c} = \mathbf{V_c} \qquad \text{coils}$$

$$\mathbf{M_{vc}}\,\dot{\mathbf{I}}_\mathbf{c} + \mathbf{M_{vv}}\,\dot{\mathbf{I}}_\mathbf{v} + \dot{\mathbf{\Psi}}_\mathbf{vp} + \mathbf{R_v}\,\mathbf{I_v} = \mathbf{0} \qquad \text{vessel}$$

$$\mathbf{M_{pc}}\,\dot{\mathbf{I}}_\mathbf{c} + \mathbf{M_{pv}}\,\dot{\mathbf{I}}_\mathbf{v} + \dot{\mathbf{\Psi}}_\mathbf{pp} + R_p\,I_p = V_{no} \qquad \text{plasma}$$

Vacuum mutual inductances

Applied voltages

Time-derivatives of plasma flux at coils, vessel, and plasma

Conductor resistances

Linearized circuit equations

$$\mathbf{M_{cc}}\,\dot{\mathbf{I}}_\mathbf{c} + \mathbf{M_{cv}}\,\dot{\mathbf{I}}_\mathbf{v} + \frac{\partial \mathbf{\Psi}_\mathbf{cp}}{\partial \mathbf{I_c}}\,\dot{\mathbf{I}}_\mathbf{c} + \frac{\partial \mathbf{\Psi}_\mathbf{cp}}{\partial \mathbf{I_v}}\,\dot{\mathbf{I}}_\mathbf{v} + \frac{\partial \mathbf{\Psi}_\mathbf{cp}}{\partial I_p}\,\dot{I}_p + \mathbf{R_c}\,\mathbf{I_c} = \mathbf{V_c}$$

$$\mathbf{M_{vc}}\,\dot{\mathbf{I}}_\mathbf{c} + \mathbf{M_{vv}}\,\dot{\mathbf{I}}_\mathbf{v} + \frac{\partial \mathbf{\Psi}_\mathbf{vp}}{\partial \mathbf{I_c}}\,\dot{\mathbf{I}}_\mathbf{c} + \frac{\partial \mathbf{\Psi}_\mathbf{vp}}{\partial \mathbf{I_v}}\,\dot{\mathbf{I}}_\mathbf{v} + \frac{\partial \mathbf{\Psi}_\mathbf{vp}}{\partial I_p}\,\dot{I}_p + \mathbf{R_v}\,\mathbf{I_v} = \mathbf{0}$$

$$\mathbf{M_{pc}}\,\dot{\mathbf{I}}_\mathbf{c} + \mathbf{M_{pv}}\,\dot{\mathbf{I}}_\mathbf{v} + \frac{\partial \mathbf{\Psi}_\mathbf{pp}}{\partial \mathbf{I_c}}\,\dot{\mathbf{I}}_\mathbf{c} + \frac{\partial \mathbf{\Psi}_\mathbf{pp}}{\partial \mathbf{I_v}}\,\dot{\mathbf{I}}_\mathbf{v} + \frac{\partial \mathbf{\Psi}_\mathbf{pp}}{\partial I_p}\,\dot{I}_p + R_p\,I_p = V_{n.o.}$$

Linearized response of plasma flux due to changes in external currents and bulk plasma current.

$$\mathbf{X}_{jk} = \frac{\partial \mathbf{\Psi}_{jp}}{\partial \xi_r}\frac{\partial \xi_r}{\partial \mathbf{I}_k} + \frac{\partial \mathbf{\Psi}_{jp}}{\partial \xi_z}\frac{\partial \xi_z}{\partial \mathbf{I}_k} \qquad j,k \in \{c,v,p\}$$

Outputs of a linear plasma response model

State-space representation of the dynamics

Express the linearized circuit equations in state-space form
for use with model-based control design tools

$$\delta\dot{\mathbf{x}} = \mathbf{A}(t)\,\delta\mathbf{x} + \mathbf{B}(t)\,\delta\mathbf{u}$$

Perturbed currents

$$\delta\mathbf{x} = \begin{bmatrix} \mathbf{I_c} - \mathbf{I_c}_{eq} \\ \mathbf{I_v} - \mathbf{I_v}_{eq} \\ I_p - I_{p_{eq}} \end{bmatrix}$$

Perturbed voltages

$$\delta\mathbf{v} = \begin{bmatrix} \mathbf{V_c} - \mathbf{V_c}_{eq} \\ 0 \\ 0 \end{bmatrix}$$

$$\mathbf{A}(t) = -\left[\widehat{\mathbf{M}}(t)\right]^{-1}\mathbf{R}$$

$$\mathbf{B}(t) = \left[\widehat{\mathbf{M}}(t)\right]^{-1}\mathbf{V}$$

Resistance matrix $\mathbf{R}$

Map from voltages to coils $\mathbf{V}$

Time-dependent mutual inductance matrix

$$\widehat{\mathbf{M}}(t) = \mathbf{M} + \mathbf{X}(t)$$

Vacuum mutual inductances → $\mathbf{M}$

Effective mutual inductance due to plasma motion → $\mathbf{X}(t)$

Validation of the no-plasma model

Wall model validated by comparing synthetic and measured magnetic diagnostic signals for NSTX-U vacuum shots.

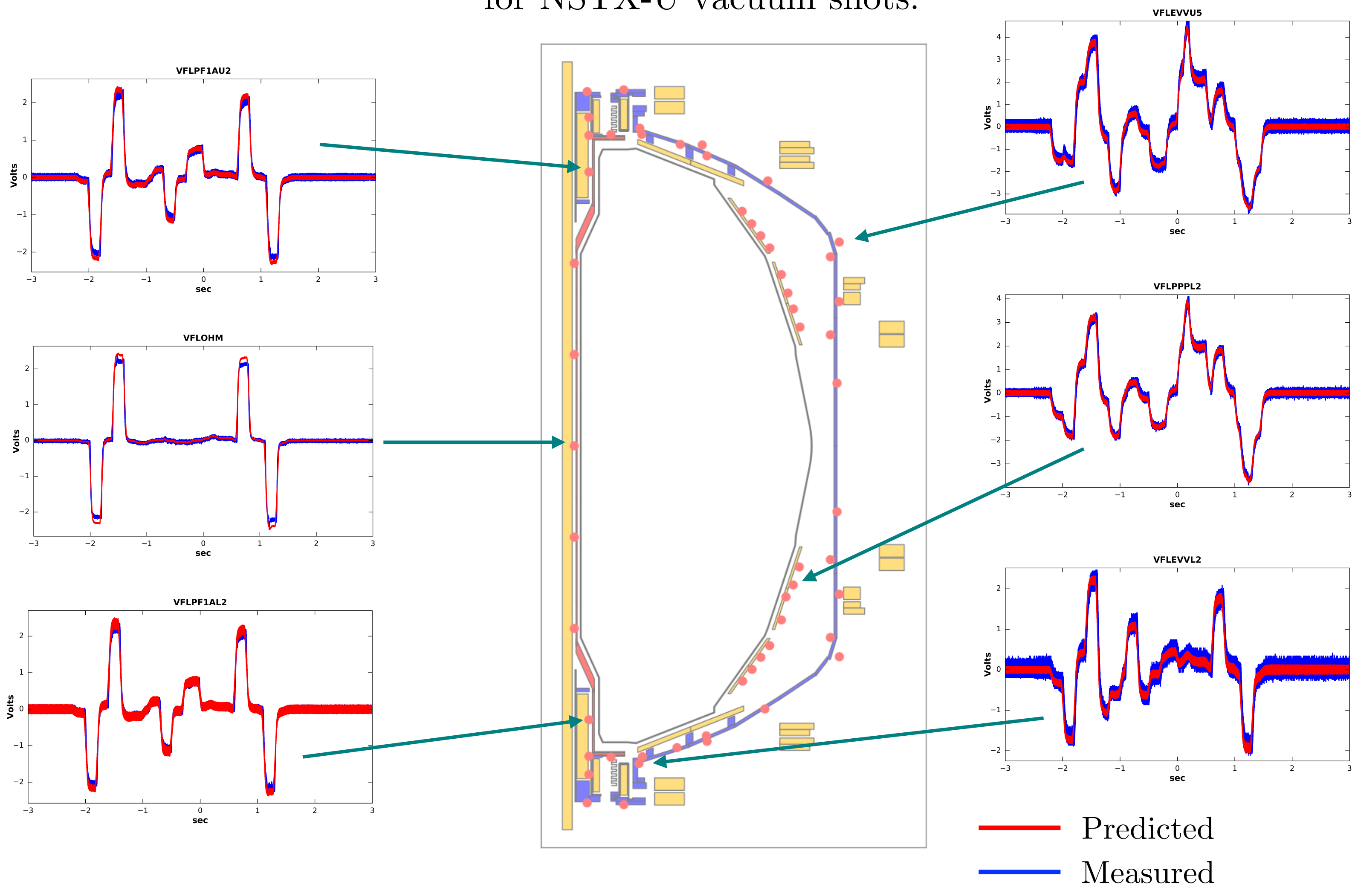

Dominant eigenmodes of the vacuum vessel

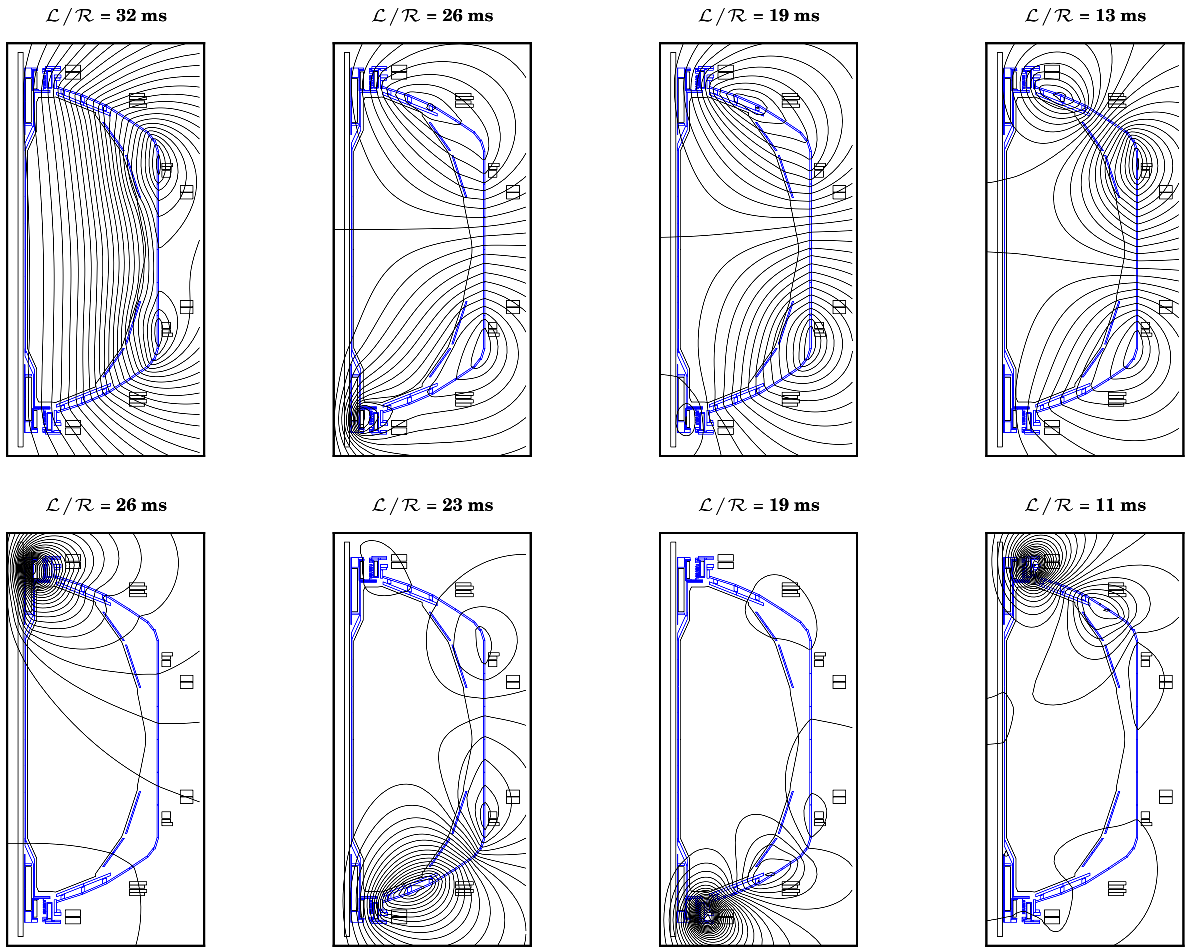

Future validation efforts will seek to identify source of the asymmetry in the vessel model.

Output equation for ISOFLUX control

State-space dynamics equation paired with output equation relating the inputs (voltages) and states (currents) to quantities of interest for control.

$$\delta \mathbf{y} = \mathbf{C}(t)\, \delta \mathbf{x} + \mathbf{D}(t)\, \delta \mathbf{u}$$

$$\delta \mathbf{y} = \begin{bmatrix} \Delta\psi_1 \\ \Delta\psi_2 \\ \Delta\psi_3 \\ \Delta r_{x_U} \\ \Delta z_{x_U} \\ \Delta r_{x_L} \\ \Delta z_{x_L} \end{bmatrix}$$

Control point fluxes ($\Delta\psi_1$, $\Delta\psi_2$, $\Delta\psi_3$)

X-point positions (Δr_{x_U}, Δz_{x_U}, Δr_{x_L}, Δz_{x_L})

$$\mathbf{C}(t) = \begin{bmatrix} \partial_{\mathbf{I}}\psi_1 \\ \partial_{\mathbf{I}}\psi_2 \\ \partial_{\mathbf{I}}\psi_3 \\ \partial_{\mathbf{I}} r_{x_U} \\ \partial_{\mathbf{I}} z_{x_U} \\ \partial_{\mathbf{I}} r_{x_L} \\ \partial_{\mathbf{I}} z_{x_L} \end{bmatrix}$$

In general, matrix entries are time-dependent.

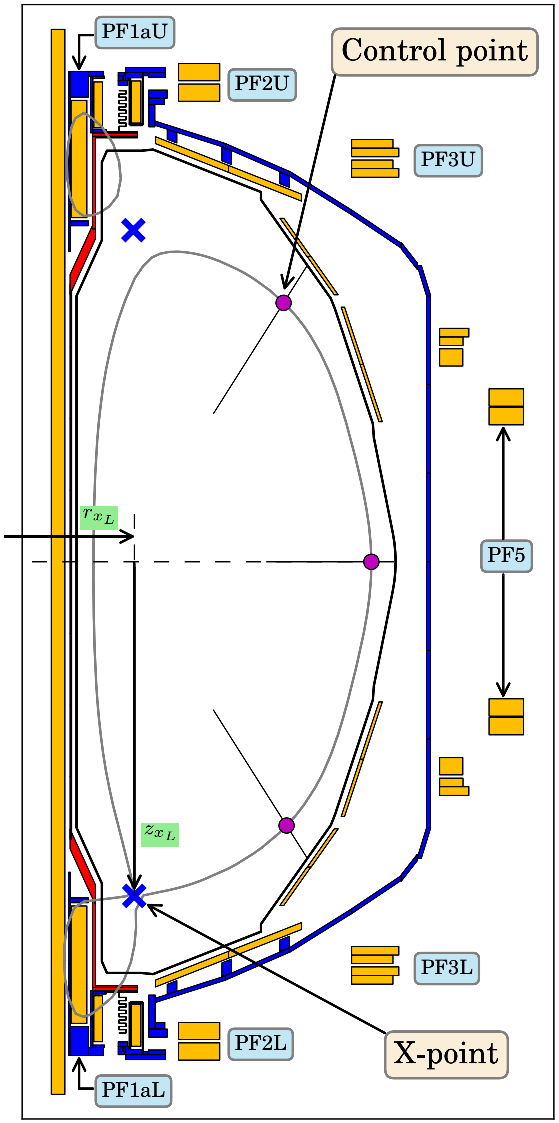

Modeling of X-point response

$$\frac{\partial r_x}{\partial \mathbf{I}} = \frac{\partial r_x}{\partial \mathbf{B}}\frac{\partial \mathbf{B}}{\partial \mathbf{I}} = \frac{\partial r_x}{\partial \mathbf{B}}\left(\left.\frac{\partial \mathbf{B}}{\partial \mathbf{I}}\right|_{\mathrm{vac}} + \frac{\partial \mathbf{B}}{\partial \xi_r}\frac{\partial \xi_r}{\partial \mathbf{I}} + \frac{\partial \mathbf{B}}{\partial \xi_z}\frac{\partial \xi_z}{\partial \mathbf{I}}\right)$$

$$\frac{\partial z_x}{\partial \mathbf{I}} = \frac{\partial z_x}{\partial \mathbf{B}}\frac{\partial \mathbf{B}}{\partial \mathbf{I}} = \frac{\partial z_x}{\partial \mathbf{B}}\left(\left.\frac{\partial \mathbf{B}}{\partial \mathbf{I}}\right|_{\mathrm{vac}} + \frac{\partial \mathbf{B}}{\partial \xi_r}\frac{\partial \xi_r}{\partial \mathbf{I}} + \frac{\partial \mathbf{B}}{\partial \xi_z}\frac{\partial \xi_z}{\partial \mathbf{I}}\right)$$

Green's functions for the coil-only vacuum fields

Outputs of a linear plasma response model

$\partial_{\mathbf{B}} r_x$ and $\partial_{\mathbf{B}} z_x$ Computed analytically using saddle-point expansion of the magnetic flux

$$x = r - r_0$$
$$v = z - z_0$$

Flux

$$(r_0 + x)\frac{\partial}{\partial x}\left(\frac{1}{r_0 + x}\frac{\partial \psi}{\partial x}\right) + \frac{\partial^2 \psi}{\partial v^2} = 0$$

Field

$$B_r = -\frac{1}{r_0 + x}\frac{\partial \psi}{\partial v} \quad B_z = \frac{1}{r_0 + x}\frac{\partial \psi}{\partial x}$$

Response of X-point position to B-field

1. Expand the flux function as a series to second-order. Solve for the series coefficients using measurements of B_r and B_z at two points.

$$\psi(x, v) = l_1 x + l_2 v + q_1 x^2 + 2 q_2 x v + q_3 v^2$$

$$B_r = -\frac{1}{r_0 + x}\left(l_2 + 2q_2 x + 2q_3 v\right)$$

$$B_z = \frac{1}{r_0 + x}\left(2(r_0 + x)q_1 + 2q_2 v + 2q_3 r_0\right)$$

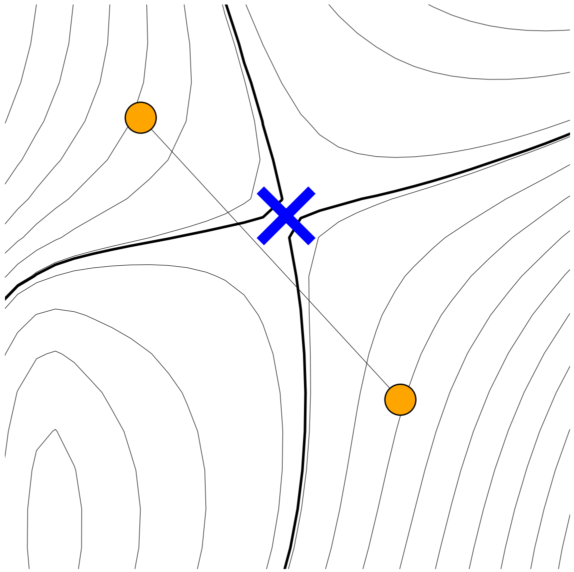

Sample points near the null

2. Solve for the (r,z) coordinates of the X-point.

$$r = r_0 + \frac{l_2 q_2 - l_1 q_3}{2\left(q_1 q_3 - q_2^2\right)} \quad z = z_0 + \frac{l_2 q_1 - l_1 q_2}{2\left(q_2^2 - q_1 q_3\right)}$$

3. Compute derivatives of (r_x, z_x) with respect to B_r and B_z.

$$\partial_{\mathbf{B}} r_x$$

$$\partial_{\mathbf{B}} z_x$$

Snowflake Shape Descriptors

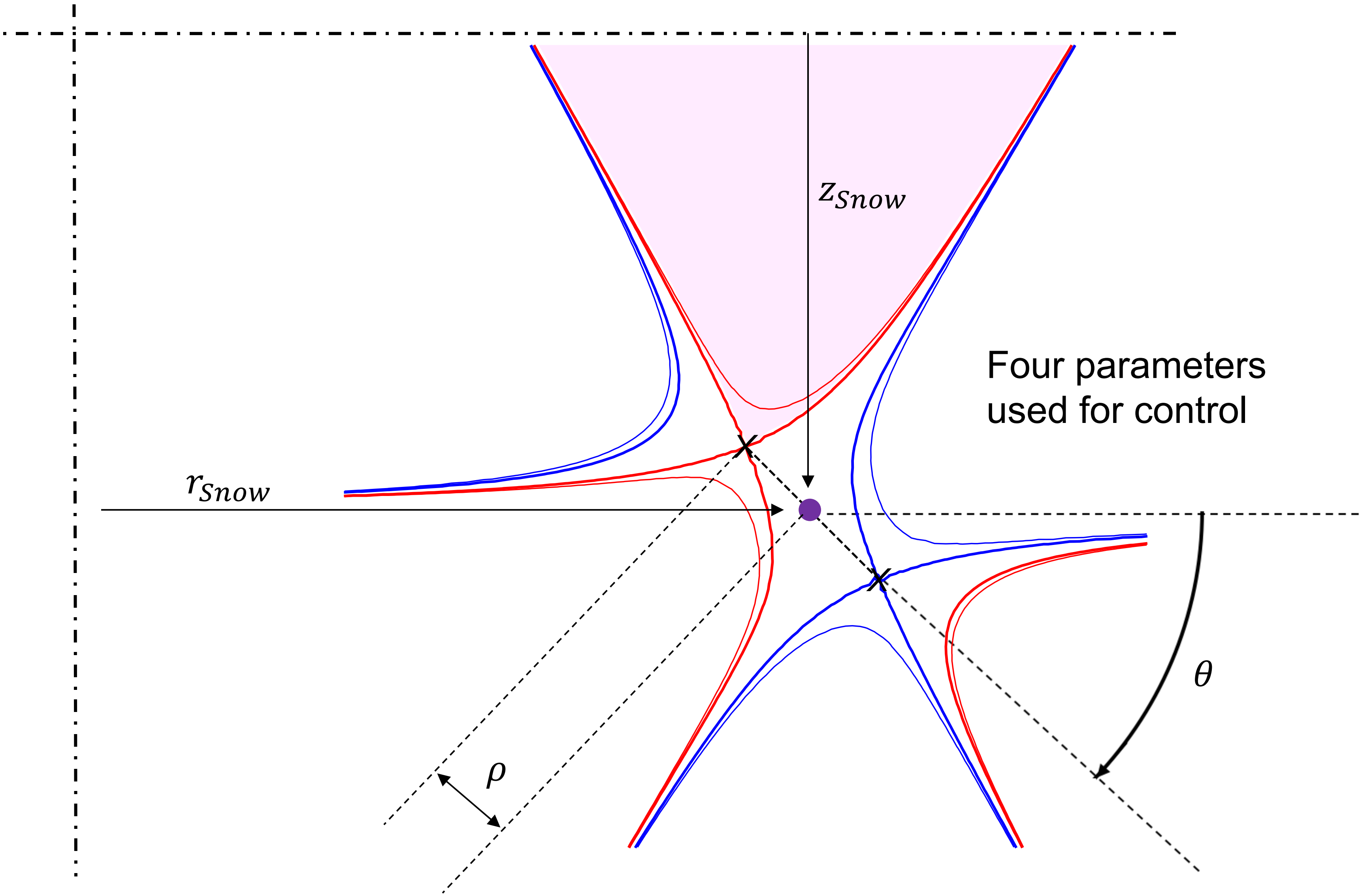

Four parameters used for control

SFD control system with PID control

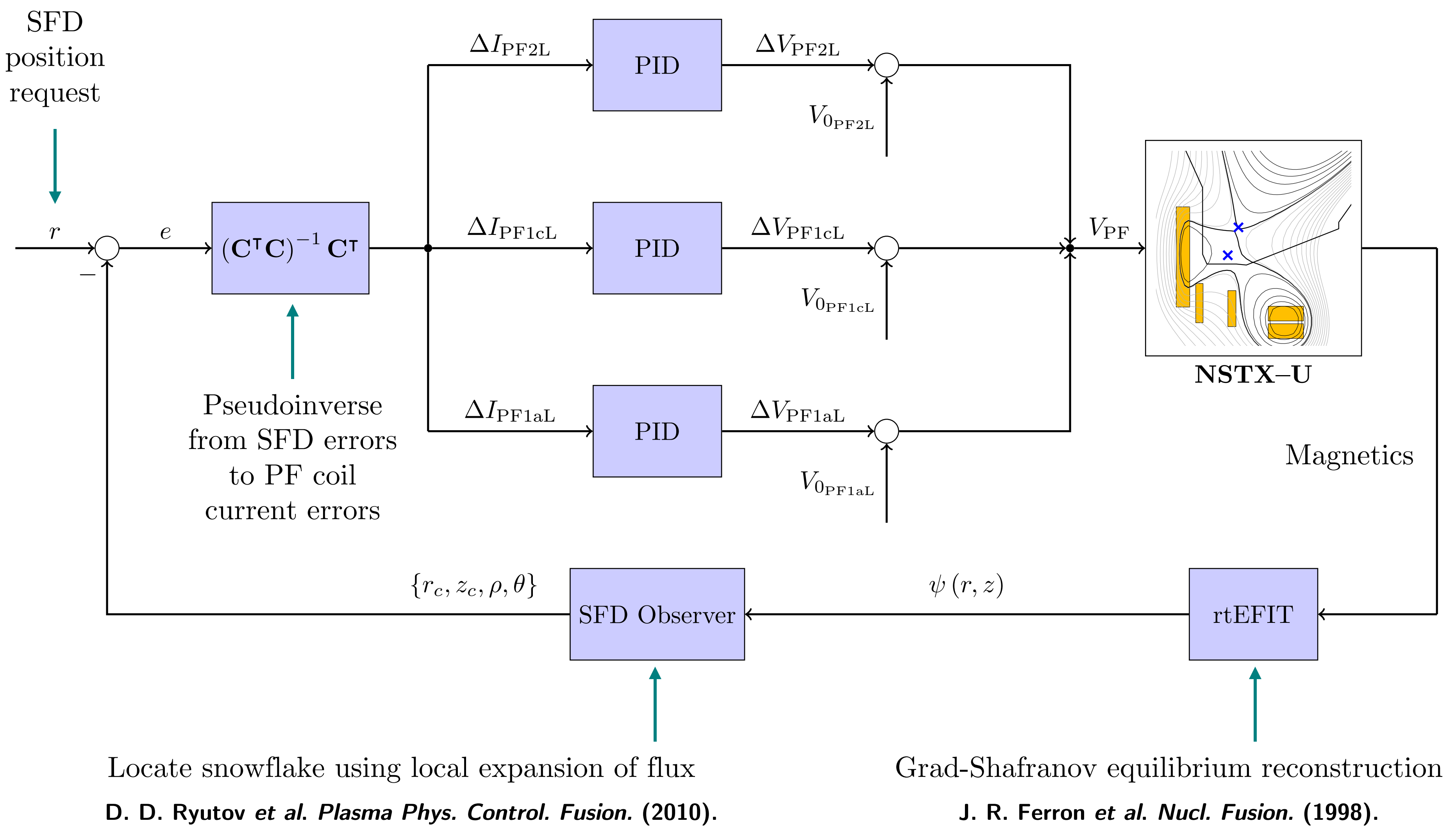

PID Control and Controller Tuning

Compute control action from the error between desired and measured signal

$$u(t) = K_{\mathrm{P}} \left(e(t) + \frac{1}{T_{\mathrm{I}}} \int_0^t e(\tau)\, d\tau + T_{\mathrm{D}} \frac{d}{dt} e(t) \right)$$

Terms proportional to error, integral of error, and derivative of error

Closed-Loop tuning of PID gains using **Relay Feedback**

Replace PID controller with relay

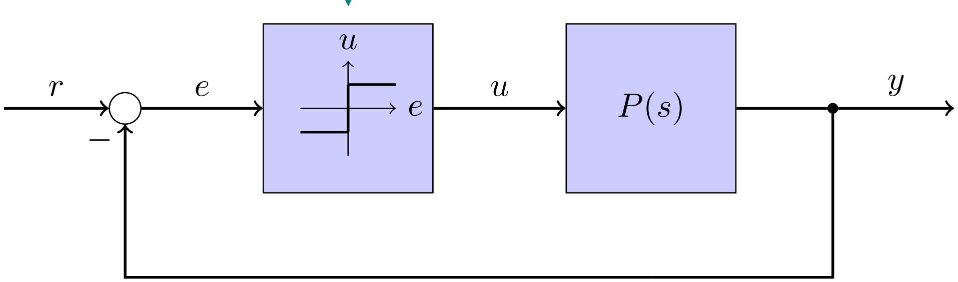

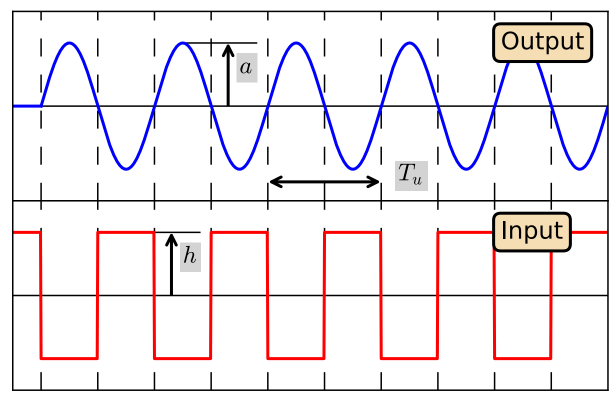

$$K_{\mathrm{u}} = \frac{4h}{\pi a}$$

Ultimate Gain

Snowflake radius scan in SFD-Minus

Scenario 1: Scan of the X-point separation in the SFD-Minus configuration.

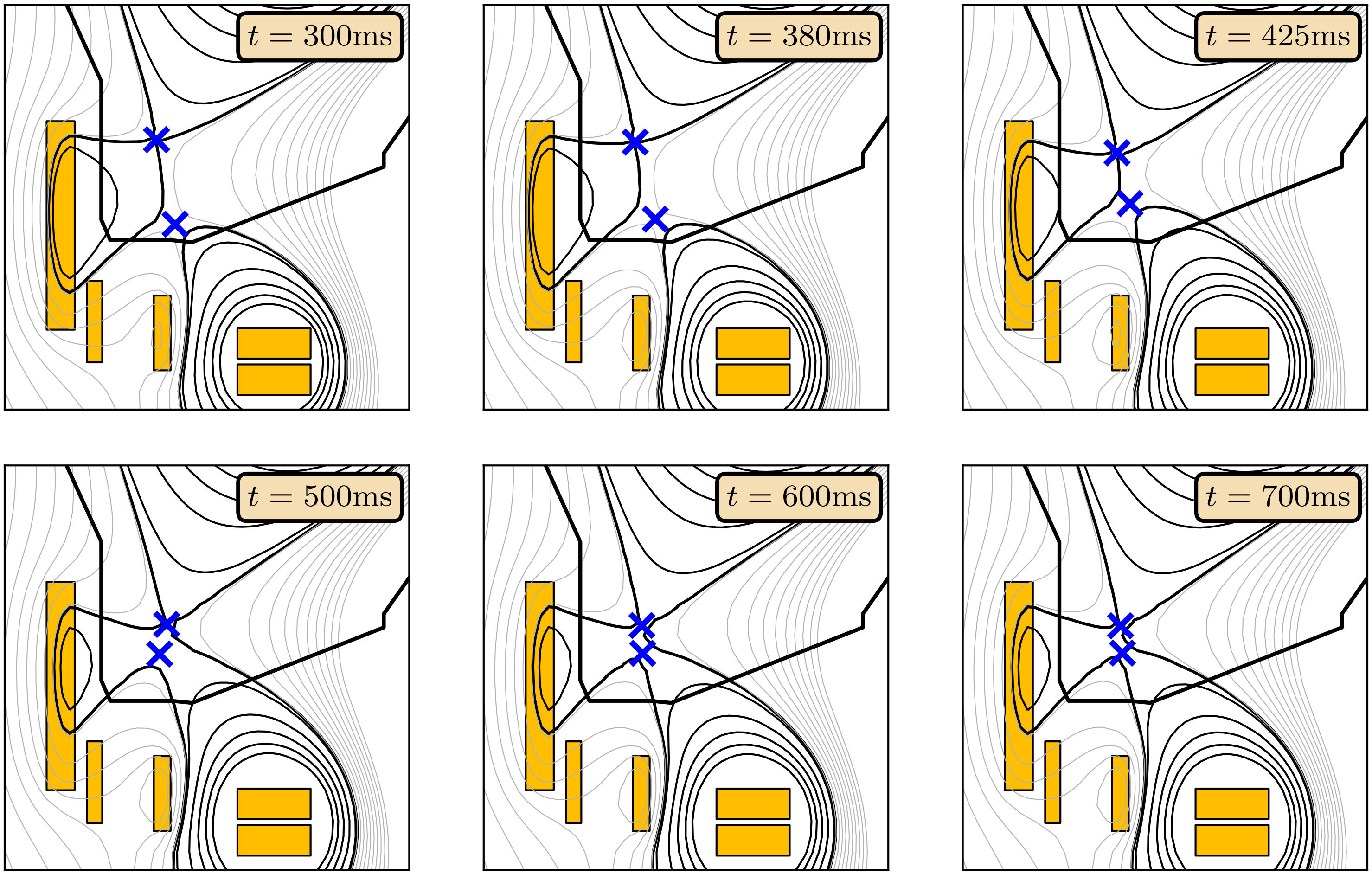

Snowflake radius scan in SFD-Plus

Scenario 2: Scan of the X-point separation in the SFD-Plus configuration.

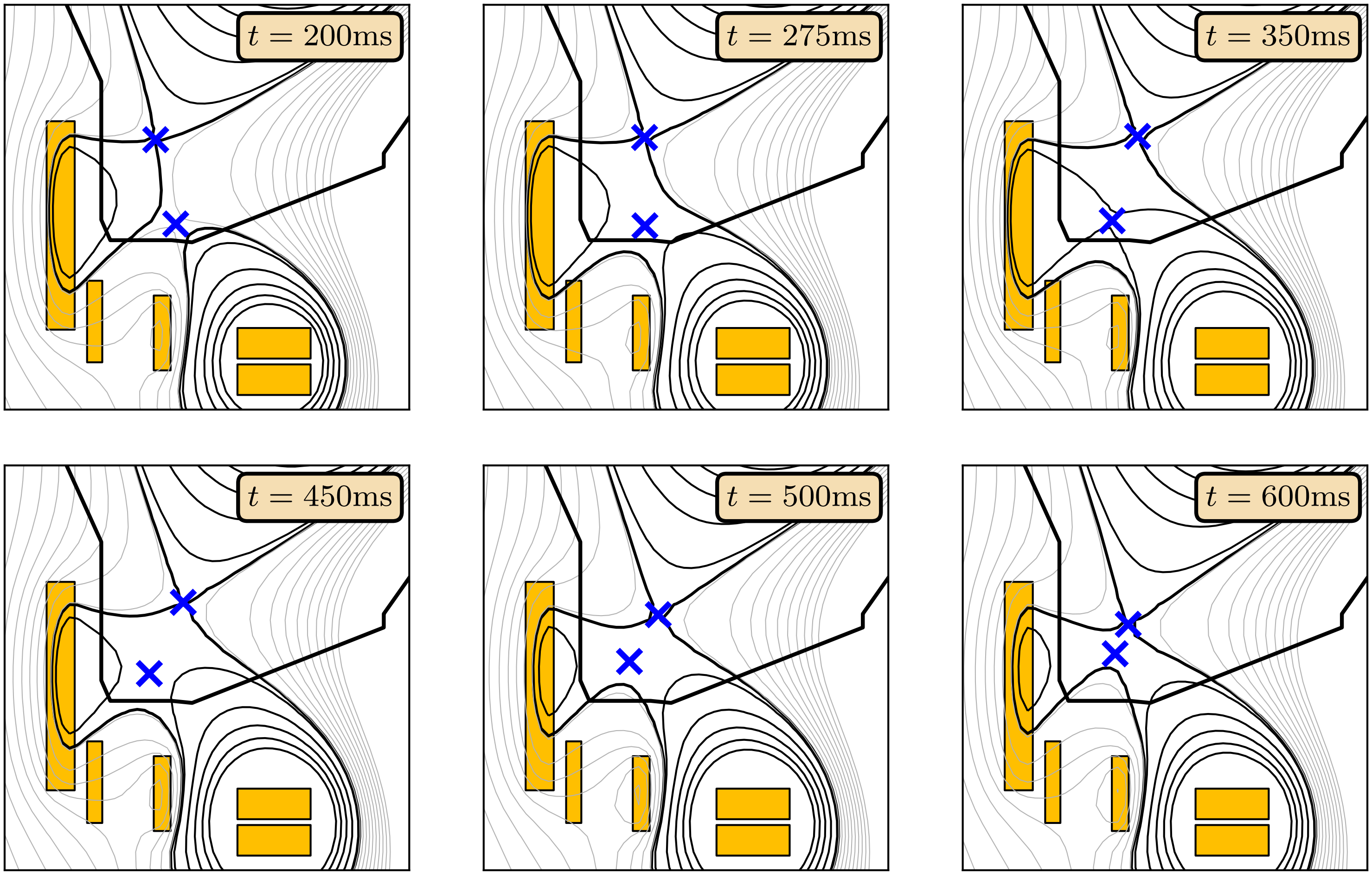

Snowflake angle scan at constant separation

Scenario 3: Scan of the angular orientation with constant X-point separation.

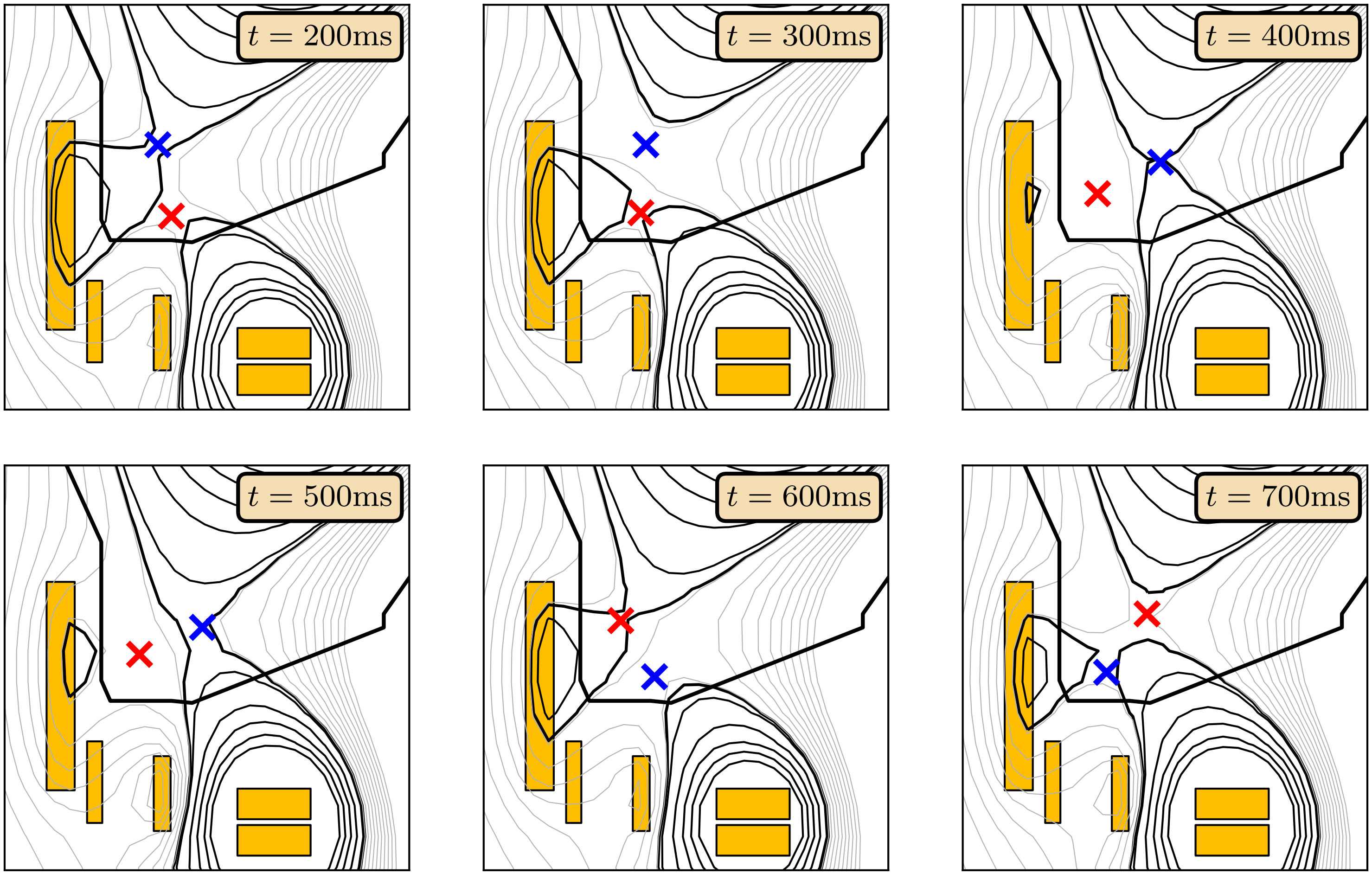

Future work

- Test the designed controllers for the SFD in-the-loop with free-boundary Grad-Shafranov equilibrium solver (for verification of controller performance).
- Integration of the SFD control into a model-based shape controller designed with LQI for reference tracking of plasma shape parameters.
- Implementation of PID-based and LQI-based controllers for the SFD in the DIII-D and NSTX-U plasma control systems.
- Test the new algorithms in DIII-D SFD scenarios.